

Double SRT Thermal Lattice Boltzmann Method for Simulating Natural Convection of Low Prandtl Number Fluids

*M. A. Wahba¹, A. A. Abdelrahman¹, N. M. El-Sahlamy², M. F. Abd Rabbo¹

¹Faculty of Engineering Shoubra, Benha University

²Nuclear and Radiological Regulatory Authority, Cairo, Egypt

Corresponding Author: *M. A. Wahba

-----ABSTRACT-----

The solution of a highly nonlinear fluid dynamics was found for low Prandtl number fluids like mercury, sodium, potassium, and sodium-potassium alloy (NaK) at different Rayleigh number to test the efficiency of an algorithm based on lattice Boltzmann method. Because the inertial force is the main domination in the flow, and the viscous effects are limited to the very thin boundary layers so there is highly nonlinear flow. The algorithm used is double SRT (single relaxation time) thermal lattice Boltzmann method. SRT method was used for a D2Q9 model for the velocity field and SRT method for a D2Q5 model for the temperature field. The results obtained are steady state solution for some cases and oscillatory solution for some other. The results are the streamlines of the velocity field, isotherm for the temperature field and Nusselt number for the heat transfer. From the simulation, we conclude that for the same Rayleigh number lower Prandtl number weak the effect of convection, make higher oscillation amplitude and make a longer period of oscillation .but for the same Prandtl number with higher Rayleigh number make more Convection effect and more time of oscillation.

Keywords: lattice Boltzmann method, low Prandtl number, natural convection, single-relaxation-time model.

Date of Submission: 01 November 2017

Date of Publication: 05 December 2017

I. INTRODUCTION

Lattice Boltzmann method evolved from Lattice Gas Cellular Automata method [1]. The first time to simulate flows by LBM was in 1988. LBM is a very efficient method for simulating flows in simple or complex geometries and several physical systems [2]. It was developed to be an alternative numerical scheme to solve the incompressible Navier-Stokes equations. Because it is easy in implementation, natural parallelism and easy treating of boundary condition it makes it easy and accurate for hydro dynamical flows. The first beginning of Thermal lattice-Boltzmann models was after the publication of McNamara and Alder paper in 1993 [3]. In this paper, a thermal lattice Boltzmann model was developed, but the method they developed need additional velocities to maintain stability. Then the passive-scalar approach by Shan [4], when they simulate two and three dimensions Rayleigh-Bénard convection using two-component lattice Boltzmann equation method. He et al [5] proposed a thermal distribution model to study thermal hydrodynamics in the incompressible limit; in his model, he introduced the simulation of the temperature field by an internal energy density distribution function. Peng et al [6] proposed a thermal energy distribution models which were simplified by removing the gradient term for the temperature. Khiabani et al [7] proposed a method in which he combined energy equation with the lattice-Boltzmann method. The hybrid method is one of the efficient ways to solve the thermal flow problems while avoiding the complications added by thermal lattice-Boltzmann method [8]. Lattice Boltzmann method is used for applications that involve multi phase flows [9–11], also Lattice Boltzmann method is capable for implementations on parallel processors such as graphics processing units [12]. In Lattice Boltzmann method there are mainly two types of collision operator. The first is BGK model based on a single relaxation time (SRT) this model was proposed by Bhatnagar, Gross, and Krook [13], this method gets high success due to its easy implementation and the ability to do complex geometries [14–15]. The second type of collision operator called Multiple Relaxation Time (MRT) [16]. This model makes high advantages compared to the BGK model due to its stable solution at high Reynolds numbers. Liquid metals or alkali metals (highly conducting) have special features in heat transfer which we did not see in other fluids. These fluids have a high thermal conductivity which leads to low Prandtl numbers. Alkali metals [17] are perfect working fluids in heat exchangers because they have low viscosity, low density, and high thermal conductivity. Also, they have a high boiling point and a low melting point which makes it easy for us to handle them efficiently with a high temperature in the liquid state. These fluids are used efficiently as a primary coolant for Liquid Metal Fast Nuclear Reactors (LMFR). Because the metal coolants have much higher heat capacity than water, which is used in most reactor designs, they remove heat more rapidly and allow much higher power density. This makes them attractive in situations where size and weight are at a premium, like on ships and submarines. To improve cooling with water, most

reactor designs are highly pressurized to raise the boiling point, which presents safety and maintenance issues that liquid metal designs do not have. Additionally, the high temperature of the liquid metal can be used to produce vapor at higher temperature than in a water cooled reactor, leading to a higher thermodynamic efficiency. This makes them attractive for improving power output in conventional nuclear power plants.

Sodium-potassium alloy (NaK) is an alloy of sodium and potassium, which is usually liquid at room temperature. NaK containing 40% to 90% potassium by weight is liquid at room temperature [18], so it has suitable properties as working fluids in heat exchangers. Our main objective is simulating Natural Convection of Low Prandtl Number Fluids. Cavities transient natural convection was studied experimentally by Pamplin and Bolt et al [19] and Kamotani and Sahaoui et al [20] by using mercury, and by Yewell et al [21], Ivey et al [22] they used water or a glycerol-water mixture for high range Rayleigh numbers. There were temperature oscillations were observed at a low frequency for the mercury results. Inconsistent results were obtained with water and with a glycerol-water mixture. Yewell et al [21], did not get oscillations in the flow at the high Rayleigh number. But Ivey et al [22] observed oscillations in temperature at the high Rayleigh number. The low-Pr fluids numerical simulation were done in many pioneering papers, for example, natural convection was predicted for a liquid metal (Pr= 0.005) at Grashof number of 1×10^7 [23] but a critical Grashof number convection was not determined [23]. Stewart and Weinberg [24] observed that the streamlines are nearly square for high Pr number and are nearly circular for low Prandtl number (Pr = 0.013) flows. Mohamad and Viskanta et al [25] studied also the transient convective motion in a two-dimensional square cavity for low Prandtl number fluid by finite difference method for Prandtl number (0.001 to 0.01) and for Grashof numbers up to 1×10^7 . Kosec and Sarler et al [26] solved the low Prandtl number natural convection problem as a benchmark. A meshless method low Prandtl number solidification problems were solved by Kosec and Sarler et al [27]. Li et al [28] discuss the solution of low Prandtl number melting problem with double single relaxation time (SRT) model, they solve conduction and convection controlled melting problems to validate their method. Z. Li, Mo Yang, and Y. Zhang et al [29] solve the natural convection with low Prandtl number (0.001 – 0.01) by double multiple relaxation time (MRT) model. And investigate the effects of Rayleigh number and Prandtl number when the natural convection results oscillate. The objective of our work is to employ double single relaxation time (SRT) model to analyze the low Prandtl number natural convection problems. And investigate the effects of Rayleigh number and Prandtl number when the natural convection results oscillate or reach steady state.

II. PROBLEM STATEMENT

The problem we are dealing with is shown in Fig (1), the considered domain is a square shaped cavity filled with low Prandtl number incompressible fluid, with vertical left and right walls are maintained at constant but different temperatures, while the rest walls are adiabatic. For all walls, the Non-slip boundary condition is applied. The problem of natural convection is solved by applying Boussinesq assumption. The description of the problem will be by the following governing equations:

$$\frac{\partial U}{\partial X} + \frac{\partial V}{\partial Y} = 0 \quad (1)$$

$$\frac{\partial U}{\partial \tau} + U \frac{\partial U}{\partial X} + V \frac{\partial U}{\partial Y} = -\frac{1}{\rho} \frac{\partial P}{\partial X} + \nu \left(\frac{\partial^2 U}{\partial X^2} + \frac{\partial^2 U}{\partial Y^2} \right) \quad (2)$$

$$\frac{\partial V}{\partial \tau} + U \frac{\partial V}{\partial X} + V \frac{\partial V}{\partial Y} = -\frac{1}{\rho} \frac{\partial P}{\partial Y} + \nu \left(\frac{\partial^2 V}{\partial X^2} + \frac{\partial^2 V}{\partial Y^2} \right) + g\beta(T - T_m) \quad (3)$$

$$\frac{\partial T}{\partial \tau} + U \frac{\partial T}{\partial X} + V \frac{\partial T}{\partial Y} = \alpha \left(\frac{\partial^2 T}{\partial X^2} + \frac{\partial^2 T}{\partial Y^2} \right) \quad (4)$$

The boundary condition for the above equations:

$$U(X, 0) = U(X, L) = U(0, Y) = U(L, Y) = 0 \quad (5)$$

$$V(X, 0) = V(X, L) = V(0, Y) = V(L, Y) = 0 \quad (6)$$

$$\frac{\partial T}{\partial X}(X, 0) = 0, \quad \frac{\partial T}{\partial X}(X, L) = 0, \quad 0 < X < H \quad (7)$$

$$T(0, y) = T_h, \quad T(L, y) = T_c \quad (8)$$

$$T_m = \frac{T_h + T_c}{2} \quad (9)$$

X and Y are the distances measured along the horizontal direction and the vertical direction respectively, U and V are the velocity components in the X and Y directions respectively, T for the temperature; P for the pressure and ρ is the density; T_h and T_c are the hot temperature and cold temperature for the walls, respectively, H is the side of the square of cavity, α is the thermal conductivity, ν is the kinematic viscosity and τ is the time.

2.1. For non-dimensional variables

$$x = \frac{X}{H}, y = \frac{Y}{H}, u_c = \sqrt{g \beta (T_h - T_c) H}$$

$$, Ma = \frac{u_c}{c_s}, u = \frac{U H}{\alpha}, v = \frac{V H}{\alpha} \quad (10)$$

$$t = \frac{\alpha \tau}{H^2}, \Theta = \frac{T - T_m}{T_h - T_c}, p = \frac{p H^2}{\rho \alpha}$$

$$, Pr = \frac{\nu}{\alpha}, Ra = \frac{g \beta (T_h - T_c) H^3 Pr}{\nu^2} \quad (11)$$

Where Pr is the Prandtl number, Ra is the Rayleighnumber, Ma is the Mach number which must be lower than 0.3 for stability reasons and $c_s = \frac{1}{\sqrt{3}}$ is the speed of sound for the lattice model D2Q9, u and v are dimensionless velocities, t is dimensionless time, p is dimensionless pressure, Θ is the dimensionless temperature, u_c is the characteristic velocity and its value must not exceed 0.1 to get accurate results because it is related to Mach number The dimensionless governing equations are written as shown below:

$$\frac{\partial u}{\partial x} + \frac{\partial v}{\partial y} = 0 \quad (12)$$

$$\frac{\partial u}{\partial t} + u \frac{\partial u}{\partial x} + v \frac{\partial u}{\partial y} = -\frac{\partial p}{\partial x} + Pr \left(\frac{\partial^2 u}{\partial x^2} + \frac{\partial^2 u}{\partial y^2} \right) \quad (13)$$

$$\frac{\partial v}{\partial t} + u \frac{\partial v}{\partial x} + v \frac{\partial v}{\partial y} = -\frac{\partial p}{\partial y}$$

$$+ Pr \left(\frac{\partial^2 v}{\partial x^2} + \frac{\partial^2 v}{\partial y^2} \right) + Pr Ra \Theta \quad (14)$$

$$\frac{\partial \Theta}{\partial t} + u \frac{\partial \Theta}{\partial x} + v \frac{\partial \Theta}{\partial y} = \left(\frac{\partial^2 \Theta}{\partial x^2} + \frac{\partial^2 \Theta}{\partial y^2} \right) \quad (15)$$

The boundary condition for the above equations:

$$u(x, 0) = u(x, L) = u(0, y) = u(L, y) = 0 \quad (16)$$

$$v(x, 0) = v(x, L) = v(0, y) = v(L, y) = 0 \quad (17)$$

$$\frac{\partial \Theta}{\partial x}(x, 0) = 0, \frac{\partial \Theta}{\partial x}(x, L) = 0, \text{adiabatic walls} \quad (18)$$

$$\Theta(0, y) = 1 \text{ hot wall}, \Theta(L, y) = 0 \text{ cold wall} \quad (19)$$

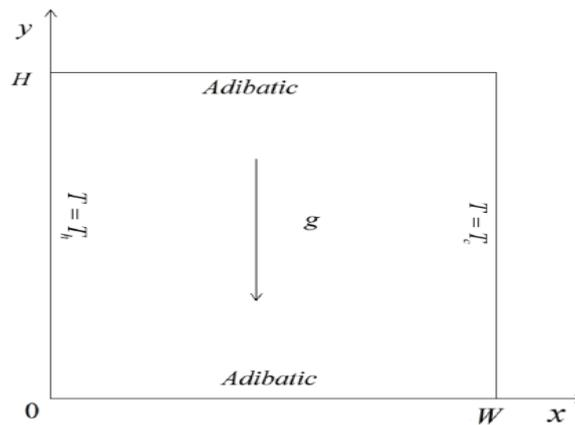


Fig (1): Natural convection model.

Nusselt number is one of the most important dimensionless numbers in heat transfer which is the ratio of convection to conduction heat transfer across the boundary.

$$Nu = \frac{h}{k/H} \Big|_{x=0} = \frac{\partial \Theta}{\partial x} \Big|_{x=0} \quad (20)$$

Where h is the convective heat-transfer coefficient and k is the thermal conductivity.

The average Nusselt number can be obtained from the following equation:

$$Nu_{ave} = \int Nu dy \quad (21)$$

Another important number is the Fourier number Fo when dealing with oscillation with time and it can be obtained from the following equation.

$$Fo = \frac{\alpha\tau}{H^2} \quad (22)$$

To make a LBM simulation with time steps t_{LBM} and a mesh size N with real time domain t_{real} and real domain H , we have to make their Fourier numbers correspond:

$$Fo = \frac{\alpha_{LBM} t_{LBM}}{N^2} = \frac{\alpha_{real} t_{real}}{H^2} \quad (23)$$

Where α_{LBM} the Lattice Boltzmann thermal conductivity and α_{real} the real thermal conductivity.

III. DOUBLE SRT THERMAL LATTICE BOLTZMANN MODEL

Double single relaxation time (SRT) thermal lattice Boltzmann model was chosen to solve the natural convection problem. D2Q9-SRT is applied to solve the velocity field and the temperature field is solved by D2Q5-SRT.

3.1 D2Q9-SRT for fluid flow

a two-dimensional model of the lattice Boltzmann model of nine discrete velocities called D2Q9 shown in Fig (2) is used for the single particle distribution functions $f_i(x,t)$ which is used to get the dynamic field simulations.

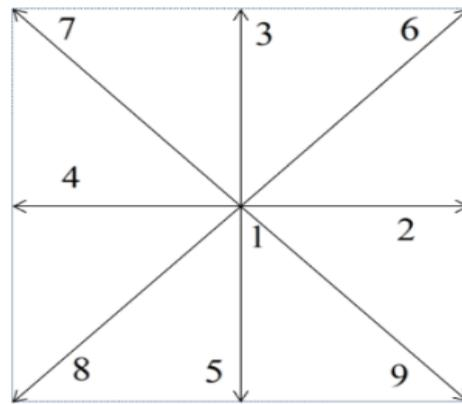


Fig (2): nine direction velocities in D2Q9 model.

The famous Bhatnagar–Gross–Krook[13] approximation for the lattice Boltzmann equation without external forces can be written as:

$$\frac{\partial f_i}{\partial t} + c_i \frac{\partial f_i}{\partial x} = \Omega(f_i)$$

$$\Omega(f_i) = -\frac{1}{\tau_v} (f_i - f_i^{eq}) \quad (24)$$

Bhatnagar-Gross-Krook et al [13] approximated the collision operator Ω , as a relaxation of the distribution functions towards the equilibrium distribution functions. And below the approximation for the lattice Boltzmann equation without external forces:

$$f_i(x + c_i \Delta t, t + \Delta t) - f_i(x, t) = \Omega(f_i) + \Delta t F_i \quad (25)$$

$$f_i(x + c_i \Delta t, t + \Delta t) - f_i(x, t) = -\frac{1}{\tau_v} (f_i(x, t) - f_i^{eq}(x, t)) + \Delta t F_i \quad (26)$$

$$\tau_v = 3\nu + 0.5 \quad (27)$$

Where ν is the lattice Boltzmann kinematic viscosity, F_i is the external force term, τ_v is the relaxation time for velocity field, f_i are the particle distribution functions defined for particle velocity vectors c_i that will be defined below for the model D2Q9 which is preferred for the velocity field.

$$c_i = (0,0) \text{ for } i = 1$$

$$c_i = (\pm 1, 0); (0, \pm 1) \text{ for } i = 2:5 \quad (28)$$

$$c_i = \text{for } (\pm 1, \pm 1) \text{ for } i = 6:9$$

x is the position and t is the time. And f_i^{eq} is the local equilibrium distribution function for the velocity field which is defined below (Ganzarolli and Milanez et al. [30]):

$$f_i^{eq}(x, t) = w_i \rho \left[1 + 3 \frac{c_i \cdot v}{c^2} + 4.5 \frac{(c_i \cdot v)^2}{c^4} - 1.5 \frac{v \cdot v}{c^2} \right] \quad (29)$$

Where w_i is the weighting factors for each direction , it is given by $w_1=4/9$, $w_{i=2:5}=1/9$, $w_{i=6:9}=1/36$ where v is macroscopic velocity, ρ is the density and c is the lattice velocity and it is given by:

$$c = \frac{\Delta x}{\Delta t} = \frac{\Delta y}{\Delta t}$$

Where Δx equals Δt equals Δy , all are set to unity and the external force is given by:

$$F_i = 3w_i\rho g\beta \frac{(T - T_m)c_i}{c^2} \quad (30)$$

The macroscopic velocity v and the density ρ can be calculated from the equation below:

$$\rho = \sum_{i=0}^8 f_i \quad , \quad \rho v(x,t) = \sum_{i=0}^8 c_i f_i(x,t) \quad (31)$$

3.2 D2Q5-SRT for the heat equation

Single relaxation time D2Q5 model is used to get the temperature field. In each node, there are five discrete velocities. Where g_i are the particle distribution functions defined for particle temperature vectors u_i that will be defined below for the model D2Q5 which is preferred for the temperature field and the model is shown in figure(3) :

$$\frac{\partial g_i}{\partial t} + u_i \frac{\partial g_i}{\partial x} = \Omega(g_i) \quad , \quad \Omega(g_i) = -\frac{1}{\tau_g}(g_i - g_i^{eq}) \quad (32)$$

$$g_i(x + u_i\Delta t, t + \Delta t) - g_i(x, t) = \Omega(g_i) \\ g_i(x + u_i\Delta t, t + \Delta t) - g_i(x, t) = -\frac{1}{\tau_g}(g_i(x, t) - g_i^{eq}(x, t)) \quad (33)$$

$$\tau_g = 3\alpha + 0.5 \quad , \quad Pr = \frac{\nu}{\alpha} \quad (34)$$

Where α is the lattice Boltzmann thermal diffusivity and τ_g is the relaxation time for temperature.

$$u_i = (0,0) \quad \text{for } i = 1 \\ , \quad u_i = (\pm 1,0); (0,\pm 1) \text{ for } i = 2:5 \quad (35)$$

The temperature equilibrium distribution functions g_i^{eq} can be taken first order (Mohamad et al [31]).

$$g_i^{eq}(x, t) = w_i T \left[1 + 3 \frac{u_i \cdot v}{c^2} \right] \quad (36)$$

Where w_i is the weighting factors for each direction and it is given by $w_{i=1}=1/3$, $w_{i=2:5}=1/6$, where v is macroscopic velocity, T is the temperature. And the dimensionless temperature can be defined as:

$$\Theta = \sum_{i=0}^5 g_i \quad (37)$$

IV. BOUNDARY CONDITIONS.

4.1 Flow Boundary conditions.

Simple bounce-back boundary conditions are used in all solid boundaries. It means that incoming boundary populations are equal to outgoing populations after the collision. Only three distribution functions needed to be computed in each wall and the rest distribution functions were computed from the streaming process. The following conditions are imposed on all boundaries:

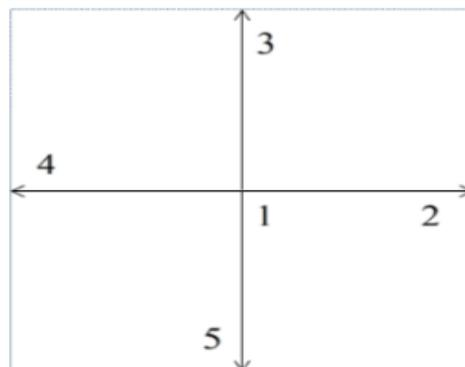


Fig (3): five direction velocities in D2Q5 model.

left wall $f(2,n)=f(4,n)$, $f(6,n)=f(8,n)$, $f(9,n)=f(7,n)$

right wall $f(4,n)=f(2,n)$, $f(8,n)=f(6,n)$, $f(7,n)=f(9,n)$

(38)

south wall $f(3,n)=f(5,n)$, $f(6,n)=f(8,n)$, $f(7,n)=f(9,n)$
 north wall $f(5,n)=f(3,n)$, $f(8,n)=f(6,n)$, $f(9,n)=f(7,n)$

Where n is the lattice on the boundary.

4.2 Temperature boundary condition.

The natural convection problem under studying has only two types of boundary conditions: constant temperature and adiabatic. After streaming process for the temperature distribution functions g_i in all boundaries, only one unknown of them has to be found. For adiabatic boundary, if x_f is the fluid node adjacent to the boundary and the energy distribution function $g_i(x_f, t)$ is unknown and has to be found but we have found from the streaming process the value of the energy distribution function $g_i^-(x_f, t)$ in the opposite direction so:

$$g_i(x_f, t) = g_i^-(x_f, t) \tag{39}$$

We use here the same boundary condition for the energy distribution function which was proposed by Tang et al. [32, 33] when he uses three kinds of thermal boundary condition encountered in practical applications.

In our study for the known temperature on the left and right walls will be like that:

For the left wall the unknown distribution function.

$$g_2 = 1 - (g_1 + g_3 + g_4 + g_5) \tag{41}$$

For the right wall the unknown distribution function.

$$g_4 = 0 - (g_1 + g_2 + g_3 + g_5) \tag{42}$$

IV. RESULTS AND DISCUSSIONS

For $Pr = 0.005$, $Ra = 15000$ results shown in Figure (4) show that the streamlines are almost circular shape, with one circulation and there might be weak circulations at the corners. There are negative streamline values which indicate clockwise circulation, which is shown in Figure (4) which indicates the effect of Prandtl number on the isotherms. Figure (4) present our data agreeing with the results of Mohamad et al. [25] which is shown in Figure (5). The time history of Nusselt number is shown in Figure (6) and the average Nusselt number oscillates around 2.1 which is shown clearly in Figure (6) but this not agree with Mohamad et al. [25] because, he said it will reach 2.1013 but without oscillation but this might because he used grid 81×81 and I used grid 182×182 but the main number 2.1 is the same.

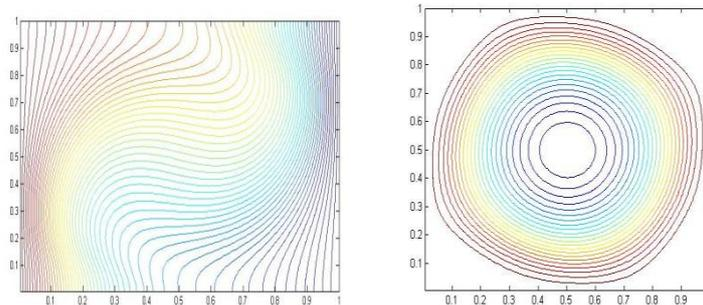


Fig (4): Isotherms and Streamlines for $Pr = 0.005$, $Ra = 15000$, present work.

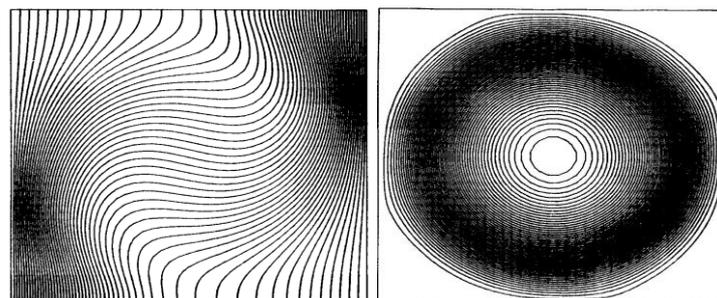


Fig (5): Isotherms and Streamlines for $Pr = 0.005$, $Ra = 15000$ Mohamad et al [25] .

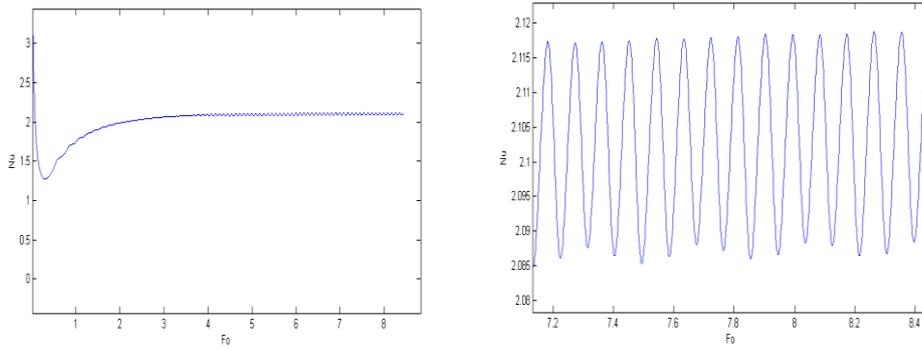


Fig (6): Time series of the average Nusselt number at left wall for $Pr=0.005$ and $Ra = 15000$.

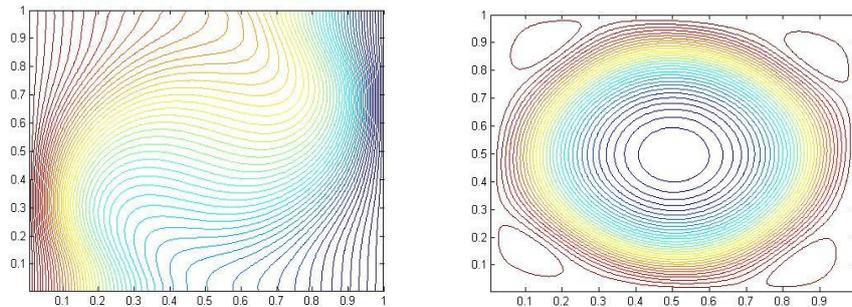


Fig (7): Isotherms and Streamlines for $Pr =0.005$, $Ra = 25000$, present work.

For $Pr =0.005$, $Ra = 25000$ results shown in Figure (7) & (9). From Figure (9) the average Nusselt number oscillates around 2.325 and this number is close to what Mohamad et al. [25] found (average $Nu =2.321$) and also the flow field with time. The corner circulations are shown in Figure (7) and these circulations change shape and position with time as observed from the oscillation. Figure (9) show that the oscillations strength increases with the Nusselt number.

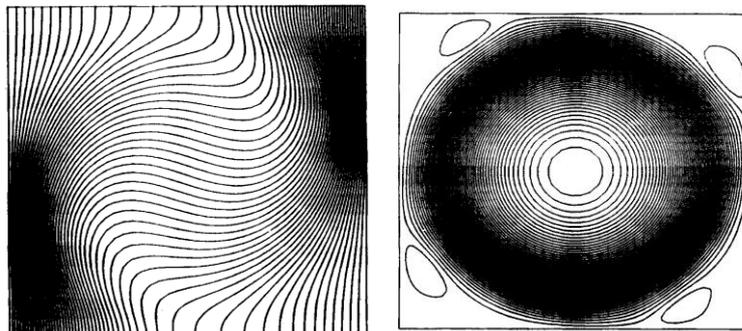


Fig (8): Isotherms and Streamlines for $Pr =0.005$, $Ra = 25000$ Mohamad et al. [25].

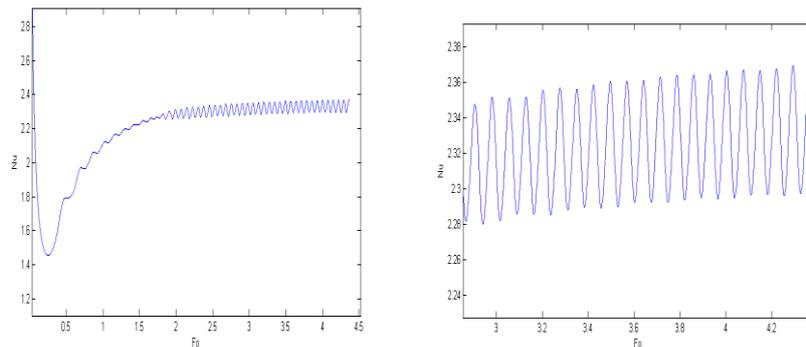


Fig (9): Time series of the average Nusselt number at left wall for $Pr=0.005$ and $Ra = 25000$.

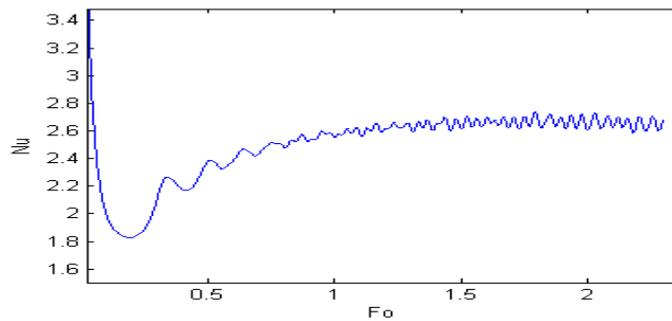


Fig: (10) Time series of the average Nusselt number at left wall for $Pr=0.005$ and $Ra = 50000$.

For $Pr = 0.005$, $Ra = 50000$ results shown in Figures (10) & (11) & (12). The figures show that there is an oscillatory solution, the average Nusselt number against Fourier number (Fo) is shown in Figure (10), it oscillates around 2.66 which give a good result as compared with (Z. Li, Mo Yang, and Y. Zhang et al. [29]) when they give average Nusselt number oscillates around 2.65. Figure (11) show that there is small vortex in the center which is rotating and changing position with time. Figure (12) show the isotherm of the model with different time which indicating change in the isotherm at the position of the small vortex.

For $Pr=0.01$ and $Ra = 10000$, the results are shown in Figures (13) & (14). Figure (13) show the streamline and the isotherm of the model, there is no oscillation in that model, there is one vortex at the center due to the effect of convection and that agree with Kosec and Sarler et al [26] and Z. Li, Mo Yang, and Y. Zhang et al [29]. Figure (14) show the Time series of the average Nusselt number at left wall, the model reaches the steady state and reaches a value 1.962 which is close to 1.95 which was done by

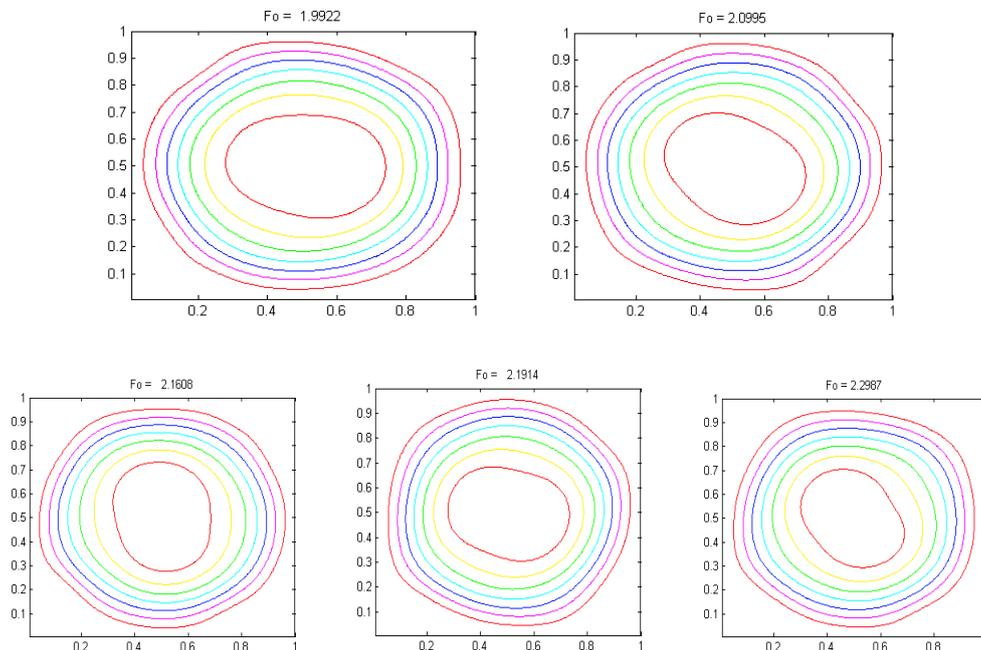
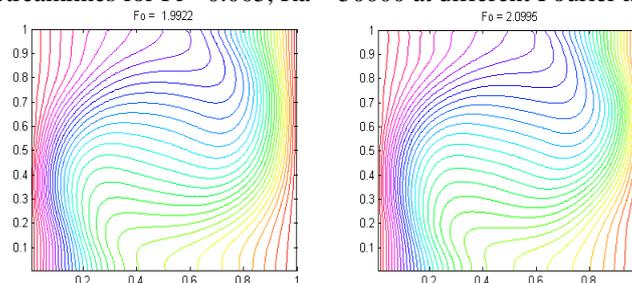


Fig (11): Streamlines for $Pr = 0.005$, $Ra = 50000$ at different Fourier number (Fo).



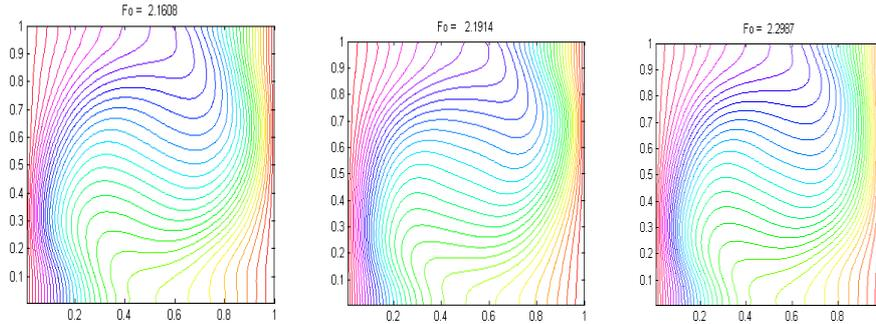


Fig (12): Isotherms for $Pr = 0.005$, $Ra = 50000$ at different Fourier number (Fo).

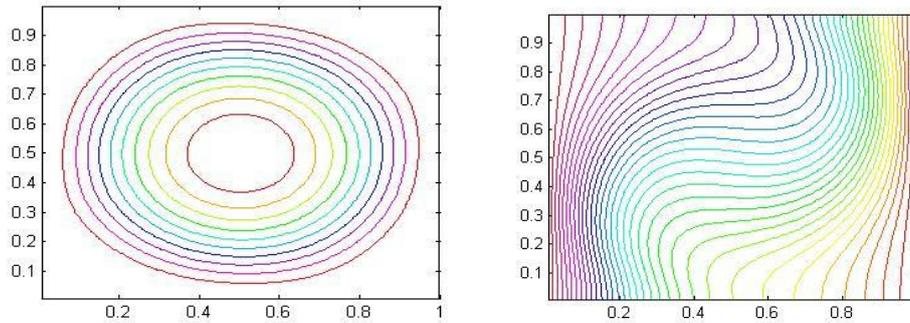


Fig (13): Streamlines and isotherms for $Pr = 0.01$, $Ra = 10000$.

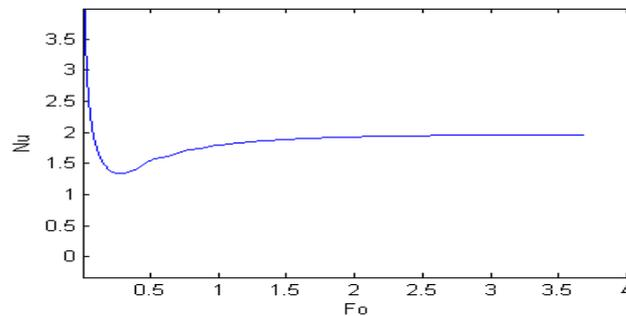


Fig (14): Time series of the average Nusselt number at left wall for $Pr = 0.01$ and $Ra = 10000$.

Z. Li, Mo Yang, and Y. Zhang et al. [29] and also to that of Kosec and Sarler et al [26]. For $Pr = 0.01$ and $Ra = 50000$, it is different from the previous case where the oscillation occurs in the solution and it is shown clearly in streamline in Figure (15) more than in the isotherm for temperature in Figure (16) for different Fourier number (Fo), where the small vortex at the center rotates clockwise direction.

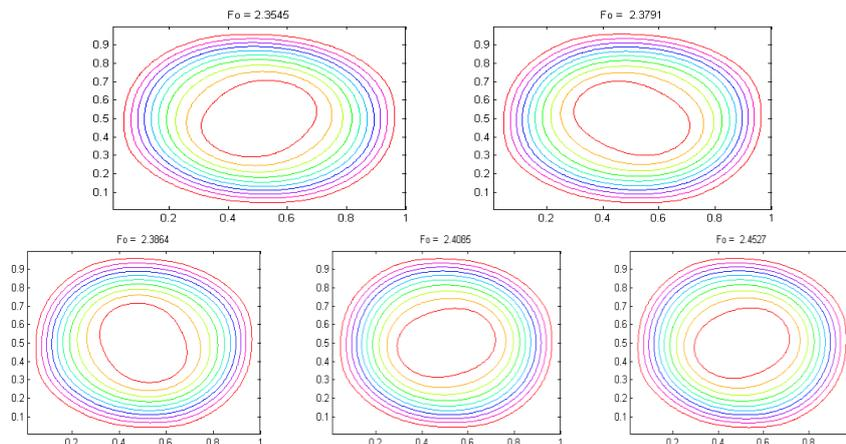


Fig (15): Streamlines for $Pr = 0.01$, $Ra = 50000$ at different Fourier number (Fo).

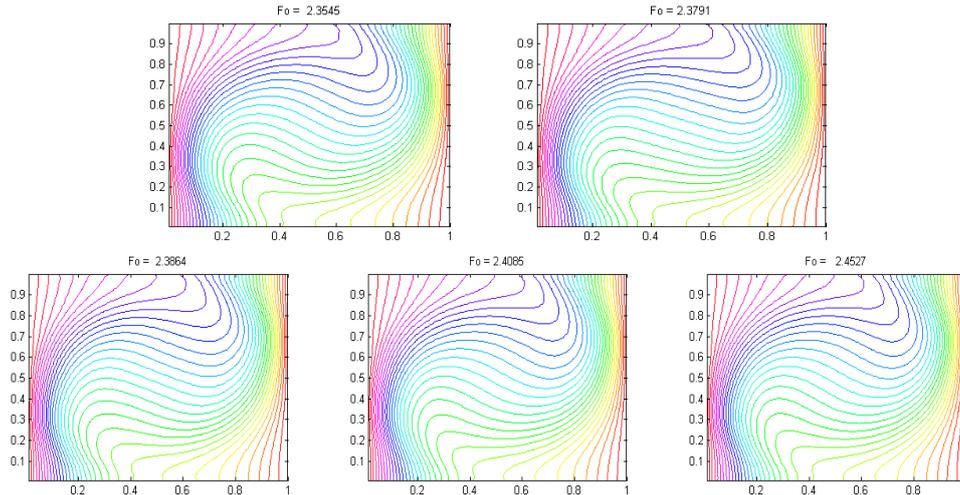


Fig (16): Isotherms for $Pr = 0.01$, $Ra = 50000$ at different Fourier number (Fo).

And the vortex changes position with time that leads to temperature field changing with times also. Figure (17) shows the variation of the average Nusselt number with different Fourier number (Fo) and from the figure, it is clear that the Nusselt number oscillates around 2.8 which was done by Z. Li, Mo Yang, and Y. Zhang et al. [29] And also agree in a close range to that of Kosec and Sarler et al. [26].

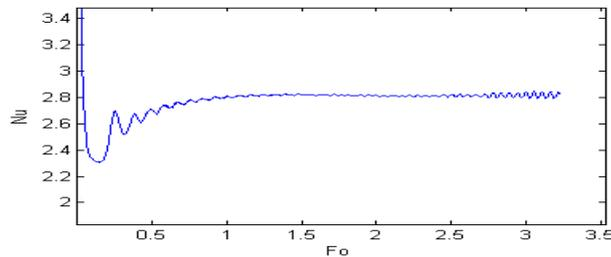


Fig (17): Time series of the average Nusselt number at left wall for $Pr=0.01$ and $Ra = 50000$.

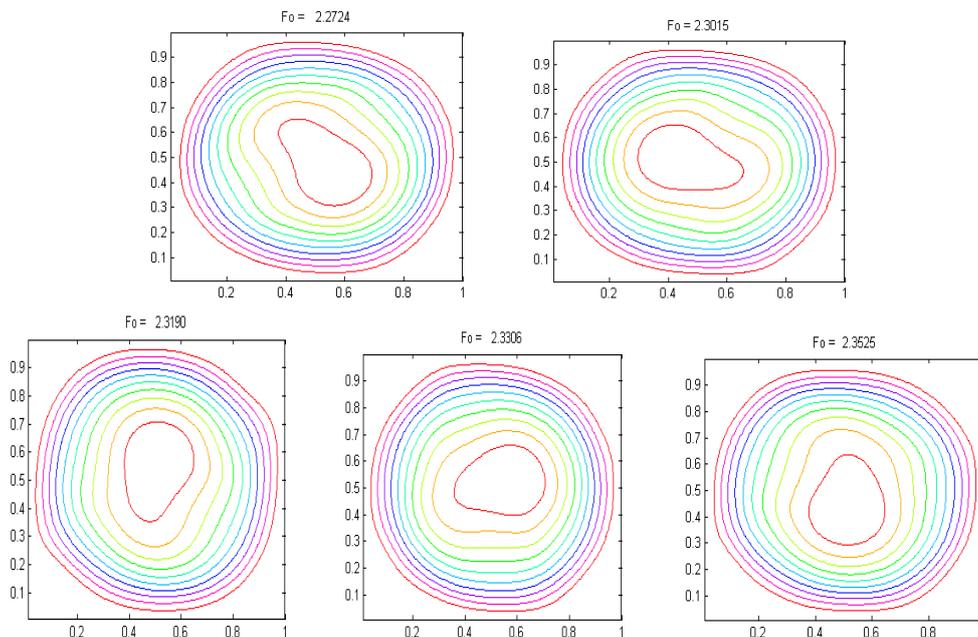


Fig (18): Streamlines for $Pr = 0.01$, $Ra = 100000$ at different Fourier number (Fo).

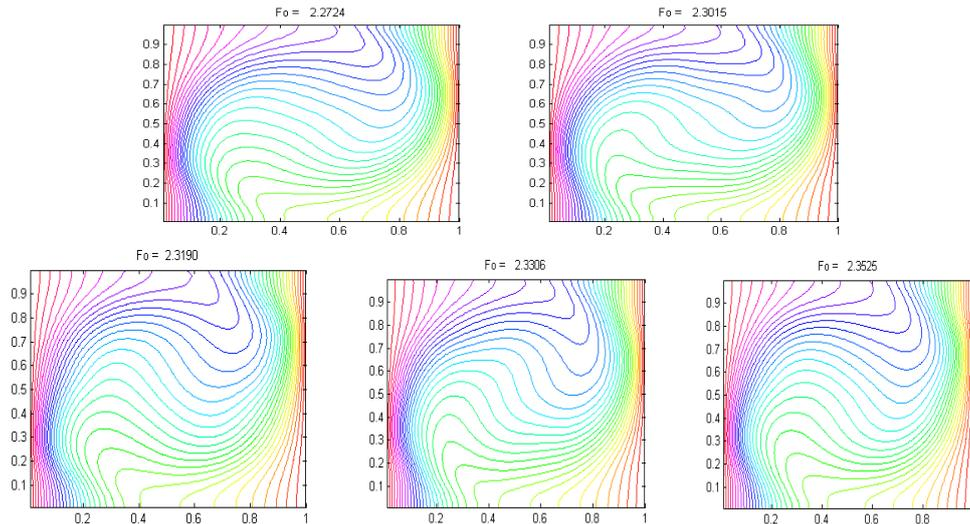


Fig (19): Isotherms for $Pr = 0.01$, $Ra = 100000$ at different Fourier number (Fo).

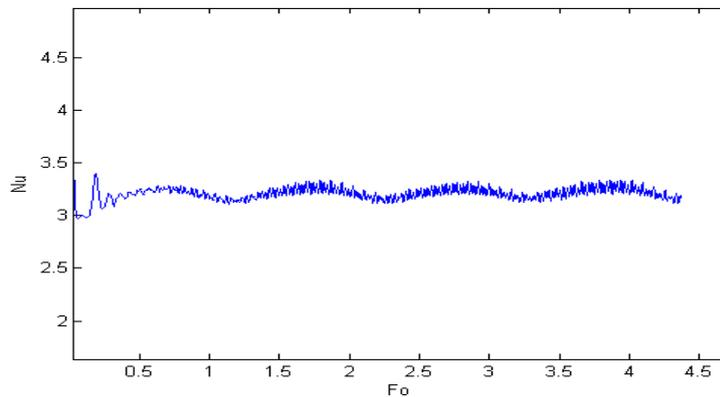


Fig (20): Time series of the average Nusselt number at left wall for $Pr = 0.01$ and $Ra = 100000$.

To study more the effects of high of Rayleigh number on the natural convection simulation was done for $Pr = 0.01$ and $Ra = 100000$. This case also has oscillatory solution but in this case, it oscillates a round a wave and that is shown in Figure (20) which represent the average Nusselt number with different Fourier number (Fo) which agree with that done by Z. Li, Mo Yang, and Y. Zhang et al. [29]. Figure (18) show the streamlines number with different Fourier number (Fo) and the figure shows the rotation of the vortex at the center of the cavity with time. Figure (19) show the isotherm of the temperature with different Fourier number (Fo) but it is clear that the changing with streamline is more than that of the isotherm which agree with that done by Z. Li, Mo Yang, and Y. Zhang et al. [29].

The last simulation was done with an important liquid which is sodium-potassium alloy. Which is made of two alkali-metals sodium (Na) and potassi-um (K), which is usually liquid at room temperature. This liquid has many important applications like in nuclear reactor and in heat exchanger. Prandtl Number of sodium– potassium alloy was taken as $Pr = 0.054$ in our simulation.

For $Pr = 0.054$, $Ra = 5400$, the results are shown in Figures (21) & (22). Figure (21) show the streamline and the isotherm of the model and there is no oscillation in that model, there is one vortex at the center due to the effect of convection and that agree with S.Saravanan and P. Kandaswamy et al [17]. It can be seen from Figure (22) which represents the Time series of the average Nusselt number at the left wall that the model reaches the steady state and reaches a value 1.768 which is close to 1.7751 which was done by S.Saravanan and P. Kandaswamy et al [17].

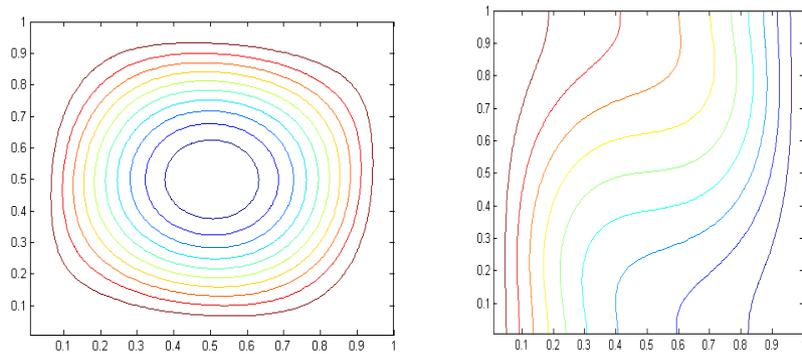


Fig (21): Streamlines and isotherms for $Pr = 0.054$, $Ra = 5400$.

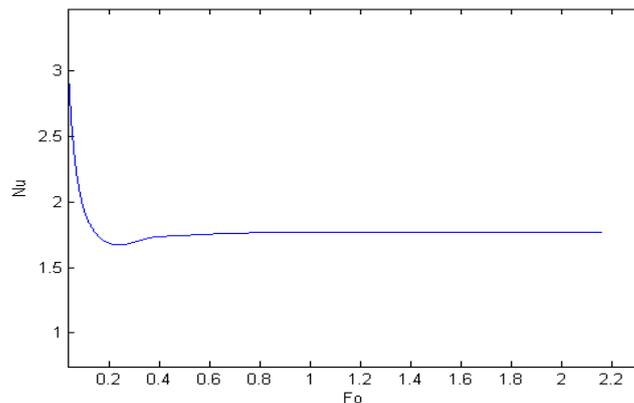


Fig (22): Time series of the average Nusselt number at left wall for $Pr = 0.054$, $Ra = 5400$.

For $Pr = 0.054$, $Ra = 10800$, the results are shown in Figures (23) & (24) & (25). Figure (23) show the streamline and the isotherm of the model, there is no oscillation in that model and there is one vortex at the center and that agree with S.Saravanan and P. Kandaswamy et al [17] as we see in their results which are shown in Figures (24). Figure (25) show the Time series of the average Nusselt number at left wall, the model reaches the steady state and reaches a value 2.1472 which is close to 2.1493 which was done by S.Saravanan and P. Kandaswamy et al [17].

For $Pr = 0.054$, $Ra = 100000$, the results are shown in Figures (26) & (27).]. It can be seen from Figure (26) the streamline and the isotherm of the model and there is no oscillation in that model and there is one vortex at the center.

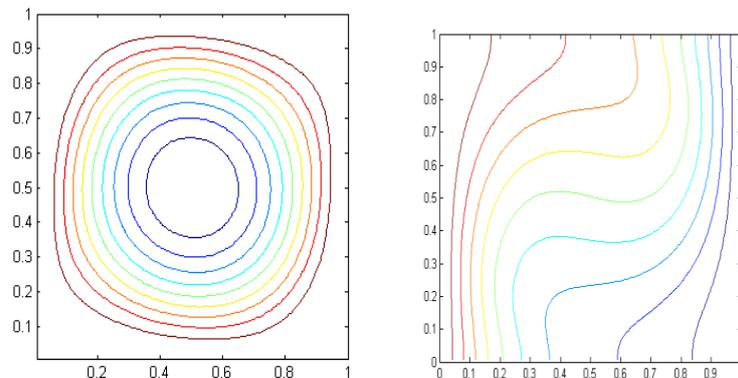


Fig (23): Streamlines and isotherms for $Pr = 0.054$, $Ra = 10800$, present work.

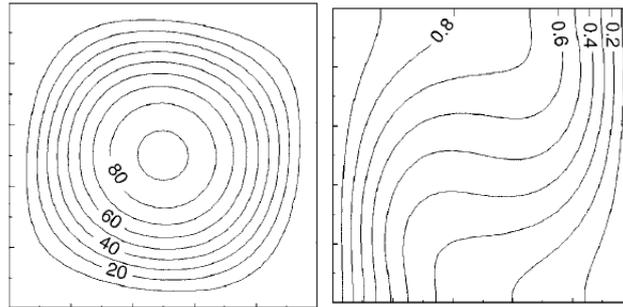


Fig (24): Streamlines and isotherms for $Pr = 0.054$, $Ra = 10800$ S.Saravanan and P. Kandaswamy [17].

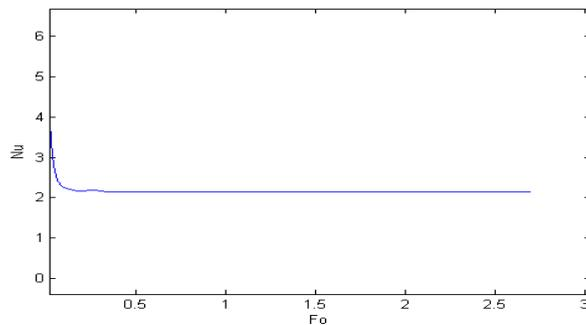


Fig (25): Time series of the average Nusselt number at left wall for $Pr = 0.054$, $Ra = 10800$.

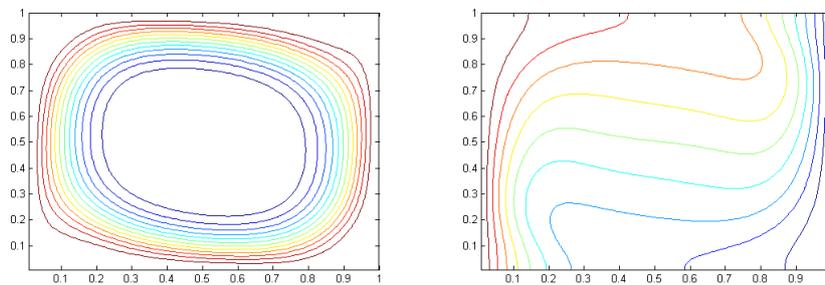


Fig (26): Streamlines and isotherms for $Pr = 0.054$, $Ra = 100000$.

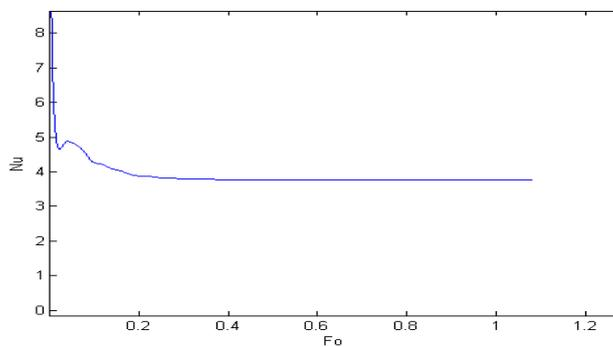


Fig (27): Time series of the average Nusselt number at left wall for $Pr = 0.054$, $Ra = 100000$.

Figure (27) show the Time series of the average Nusselt number at the left wall that the model reaches the steady state and reaches a value 3.7682. From looking at the results there increase in average Nusselt number as we increase Rayleigh number and there is a big change in the streamlines as it changes from almost a circle to a potatoes shape and also there is a big change in the isotherm shapes.

V. CONCLUSIONS

Simulation of natural convection for low Prandtl number fluids (0.005 – 0.054) by double single relaxation time lattice Boltzmann thermal model was carried out. The simulation was carried out for different cases at different Rayleigh number and the results agree with the reference results well. So we conclude that double SRT thermal LBM is valid to simulate low Prandtl number fluids.

From the results we conclude that for the same Rayleigh number lower Prandtl number weak the effect of convection, make higher oscillation amplitude and make, longer period of oscillation .but for the same Prandtl number with higher Rayleigh number make more Convection effect and more time of oscillation.

NOMENCLATURE

c lattice speed
 c_p specific heat (J/kg K)
 c_s sound speed
 c_i particle speed
 f_i density distribution
 F_i body force
 Fo Fourier number
 g_i energy distribution
 k thermal conductivity (W/m k)
 Ma Mach number
 p pressure (Pa)
 P non-dimensional pressure
 Pr Prandtl number
 Ra Rayleigh number
 τ time (s)
 T temperature K
 U velocity in x-direction (m/s)
 u_i Particle speed in energy distribution
 u non-dimensional velocity in x-direction
 V velocity in y-direction (m/s)
 v non-dimensional velocity in y-direction
 α thermal diffusivity(m²/s)
 β thermal expansion (K⁻¹)
 Θ Non-dimensional temperature
 μ Viscosity (Kg/ms)
 ρ Density(kg/m³)
 t non-dimensional time
 ν kinematic viscosity (m²/s)
 T_h hot temperature
 T_c cold temperature
 H side of the square of cavity
SRT single relaxation time
 Ω collision operator
 τ_v relaxation time for velocity field
 f_i^{eq} local equilibrium distribution function for the velocity field
 w_i is the weighting factors for each direction for velocity distribution function
 τ_g is the relaxation time for temperature
 g_i^{eq} Temperature equilibrium distribution functions
 w_{1i} is the weighting factors for each direction for temperature distribution function

REFERENCES

- [1]. G. R. McNamara and G. Zanetti, "Use of the Boltzmann equation to simulate lattice-gas automata", Phys. Rev. Lett.61,pp. 2332:2335, 1988.
- [2]. S. Chen and G. D. Doolen, "Lattice Boltzmann method for fluid flows", Annual Review of Fluid Mechanics, 30,pp.329-364, 1998.
- [3]. McNamara and Alder, "Analysis of the lattice Boltzmann treatment of hydrodynamics", Physica A, vol. 194, pp. 218-228, 1993.
- [4]. Shan, "Simulation of Rayleigh-Benard convection using a lattice Boltzmann method", in Physical Review E, vol. 55, pp. 2780-2788, 1997.
- [5]. X. He, S. Chen and G. D. Doolen, "A novel thermal model for the lattice Boltzmann method in incompressible limit", Journal of Computational Physics, vol. 146, pp. 282-300, 1998.

- [6]. Peng, Shu., and Chew, "Simplified thermal lattice Boltzmann model for incompressible thermal flows", *Phys. Rev. E*, vol. 68, p. 026701, 2003.
- [7]. Khiabani, Joshi and Aidun, "Heat transfer in micro channels with suspended solid particles: Lattice-Boltzmann based computations", Master's thesis, Georgia Institute of Technology, 2006.
- [8]. P. Lallemand, and L. Luo, "Hybrid finite difference thermal lattice Boltzmann equation", *International Journal of Modern Physics B*. Volume 17, Issue 01n02, 2003.
- [9]. X. Shan and H. Chen, "Simulation of nonideal gases and liquid-gas phase transitions by the lattice Boltzmann equation", *Phys. Rev. E* 49, 2941 – Published 1 April 1994.
- [10]. M. Sbragaglia, R. Benzi, L. Biferale, S. Succi, K. Sugiyama, and F. Toschi, "Generalized lattice Boltzmann method with multi range pseudopotential", *Phys. Rev. E* 75, 026702 – Published 8 February 2007.
- [11]. Falcucci, G. Bella, G. Chiatti, G. Chibbaro, S. Sbragaglia and M. Succi, "Lattice Boltzmann models with midrange interactions", *Communications in Computational Physics* Volume 2, Issue 6, pp. 1071-1084, December 2007.
- [12]. F. Kuznik, C. Obrecht, Gilles Rusaouen, Jean-Jacques Roux, "LBM based flow simulation using GPU computing processor", *Computers & Mathematics with Applications* Volume 59, Issue 7, pp. 2380-2392, 2010.
- [13]. P. L. Bhatnagar, E. P. Gross, and M. Krook, "A Model for Collision Processes in Gases. I. Small Amplitude Processes in Charged and Neutral One-Component Systems", *Phys. Rev.* 94, 511 – Published 1 May 1954.
- [14]. D. Chen, K. Lin, and Chao, "Immersed boundary method based lattice Boltzmann method to simulate 2d and 3d complex geometry flows", *International Journal of Modern Physics C Computational Physics and Physical Computation*. Volume 18, Issue 04, 2007.
- [15]. C. Chang, Chih-Hao Liu, and Chao-An Lin, "Boundary conditions for lattice Boltzmann simulations with complex geometry flows", *Computers & Mathematics with Applications*. Volume 58, Issue 5, pp. 940-949, 2009.
- [16]. H. Yu, L. Luo, and Sharath S. Girimaji, "LES of turbulent square jet flow using an MRT lattice Boltzmann model", *Computers & Fluids*. Volume 35, Issues 8–9, pp. 957-965, 2006.
- [17]. S. Saravanan and P. Kandaswamy, "Buoyancy Convection in Low Prandtl Number Liquids with Large Temperature Variation", *Meccanica* 37, pp. 599–608, 2002.
- [18]. https://en.wikipedia.org/wiki/Sodium_potassium_alloy#cite_note-basf-ds-NaK-2.
- [19]. B. R. Pamplin and G. H. Bolt, "Temperature oscillation, induced in a mercury bath by horizontal heat flow", *J. Phys. D. Appl. Phys.* 9, pp. 145-149, 1976.
- [20]. Y. Kamotani and T. Sahraoui, "Oscillatory natural convection in rectangular enclosures filled with mercury", in P. J. Marchal and I. Tansawa (eds), *Proc. 1987 ASME-JSME Thermal Engineering Joint Vol. 2*, ASME/JSME, New York/Tokyo, 1987, pp. 241-245.
- [21]. R. Yewell, D. Poulidakos, and A. Bejan, "Transient natural convection experiments in shallow enclosures", *J. Heat Transfer*, 104, pp. 533-538, 1982.
- [22]. G. N. Hey, "Experiments on transient natural convection in a cavity", *J. Fluid Mech.*, 144, pp. 389-401, 1984.
- [23]. P. M. Gresho and C. G. Upson, "Application of a modified finite element method to the time-dependent thermal convection of a liquid metal", in C. Taylor, C. Johnson, J. A. Smith and W. Ramsey (eds), *Proc. 3rd Int. Conf. on Numerical Methods in Laminar and Turbulent Flow*, Pineridge, Swansea, pp. 750-762, 1983.
- [24]. S. Paolucci and D. R. Chenoweth, "Transition to chaos in a differentially heated vertical cavity", *J. Fluid Mech.*, 201, pp. 379-410, 1989.
- [25]. A. Mohamad, and R. Viskanta, "Transient natural convection of low – Prandtl – number fluids in a differentially heated cavity", *International Journal for numerical methods in fluids*, VOL. 13, pp. 61-81, 1991.
- [26]. Kosec and Sarler, "Solution of a low Prandtl number natural convection benchmark by a local meshless method", *International Journal of Numerical Methods for Heat & Fluid Flow*, 23(1), pp. 189-204, 2013.
- [27]. Kosec, and Sarler, "simulation of macro segregation with Meso-segregates in binary metallic casts by a meshless method", *Engineering Analysis with Boundary Elements*, 45, pp. 36-44, 2014.
- [28]. Z. Li, M. Yang, and Y. Zhang, "Numerical Simulation of Melting Problems using the Lattice Boltzmann Method with the Interfacial Tracking Method", *Numerical Heat Transfer, Part A*, 68: 1175–1197, 2015.
- [29]. Z. Li, Mo Yang, and Y. Zhang, "Double MRT Thermal Lattice Boltzmann Method for Simulating Natural Convection of Low Prandtl Number Fluids", *Int. J. Numer. Methods Heat Fluid Flow*, 26(6), pp. 1809-1909, 2016.
- [30]. M. M. Ganzarolli and L. Milanez, "Natural convection in rectangular enclosures heated from below and symmetrically cooled from the sides", *Int. J. Heat Mass Transfer*, pp. 1063–1073, 1995.
- [31]. A.A. Mohamad, A. Kuzmin, "A critical evaluation of force term in lattice Boltzmann method natural convection problem", *International Journal of Heat and Mass Transfer* 53, pp. 990–996, 2010.
- [32]. G.H. Tang, W.Q. Tao and Y.L. He, "Thermal boundary condition for the thermal lattice Boltzmann equation", *Phys. Rev. E*, 72(1), pp. 016703, 2005.
- [33]. G.H. Tang, W.Q. Tao and Y.L. He, "Simulation of fluid flow and heat transfer in a plane channel using the lattice Boltzmann method", *Int. J. Modern Phys. B*, 17(1–2), pp. 183–187, 2003.

*M. A. Wahba. "Double SRT Thermal Lattice Boltzmann Method for Simulating Natural Convection of Low Prandtl Number Fluids." *The International Journal of Engineering and Science (IJES)*, vol. 06, no. 12, 2017, pp. 21-35.